Electronic Supplementary Material (ESI) for Nanoscale.
This journal is © The Royal Society of Chemistry 2015

SUPPORTING INFORMATION

Nanoantioxidant-driven plasmon enhanced proton-coupled electron transfer

*Georgios A. Sotiriou[1,2], Christoph O. Blattmann[1], Yiannis Deligiannakis[1,3]**

[1]Particle Technology Laboratory, Institute of Process Engineering, Department of Mechanical and Process Engineering, ETH Zurich, Sonneggstrasse 3, CH-8092, Zurich, Switzerland.
[2]Drug Formulation & Delivery, Institute of Pharmaceutical Sciences, Department of Chemistry and Applied Biosciences, ETH Zurich, Vladimir-Prelog-Weg 3, CH-8093, Zurich Switzerland.
[3]Laboratory of Physical Chemistry and Materials, Department of Physics, University of Ioannina, 45110 Ioannina, Greece.

*Corresponding author: Y. Deligiannakis, ideligia@cc.uoi.gr

22 September 2015

Submitted to: *Nanoscale*

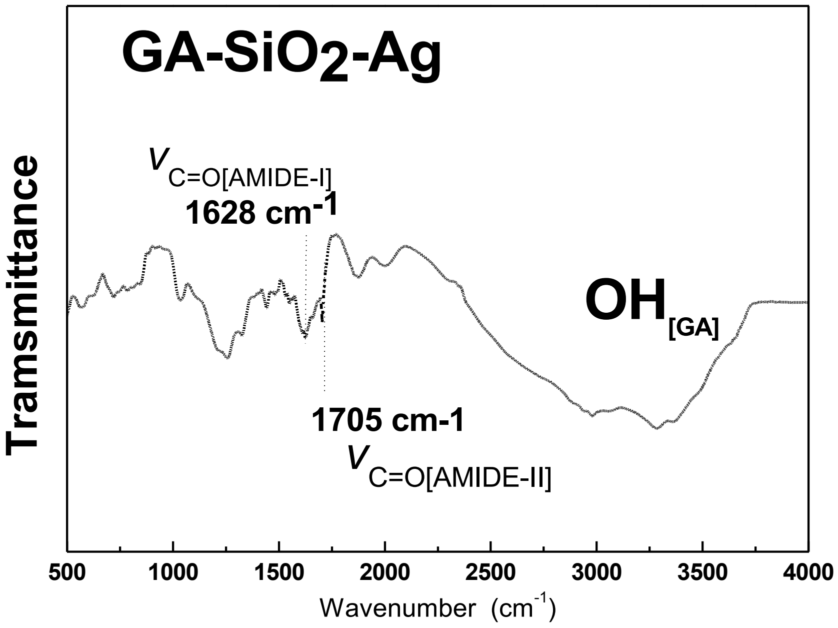

Figure S1. FTIR spectra of the gallic acid (GA) functionalized SiO_2-coated Ag nanoparticles.

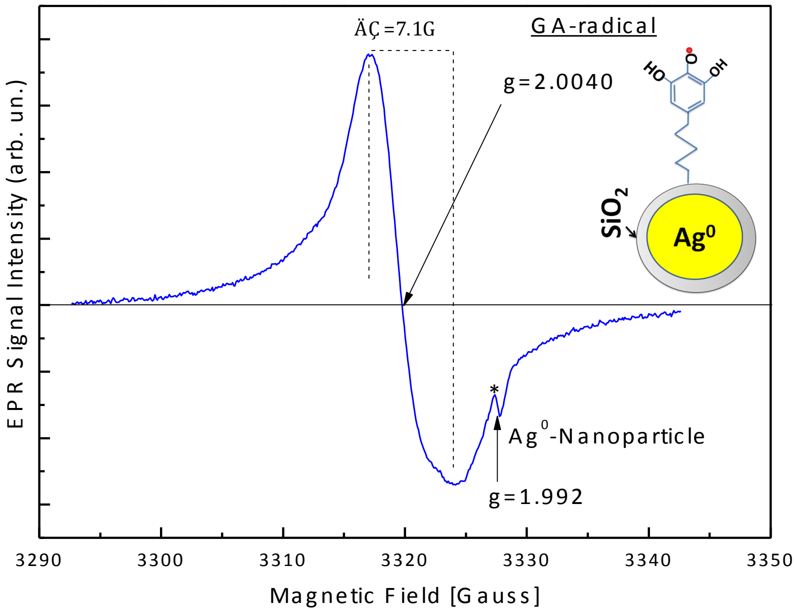

Figure S2. EPR spectrum of the GA functionalized SiO_2-coated Ag NPs in H_2O at pH 12. The radical signal with g=2.0040 is typical for monomeric GA radicals where the unpaired spin is localised on the phenolic oxygen. The small radical peak at g=1.992 is due to Ag^0 nanoparticles.

Our dynamic light scattering (DLS) data (Supporting Information, Figure S3) show that upon bulk heating there is a strong agglomeration effect. This might be attributed to GA-GA radical couplings from colliding nanoparticles, according to the following mechanism as shown previously[1]; the HAT by GA to DPPH involves the formation of a transient GA radical.[1] Thus, when the particle-particle collision kinetic rate is increased, transient GA radicals from colliding particles can couple to each other *i.e.* resulting in polymerization-induced agglomeration of nanoparticles. *Bulk heating* increases the particle-particle collision rates due to Brownian motion enhancement, thus enhanced agglomeration occurs.

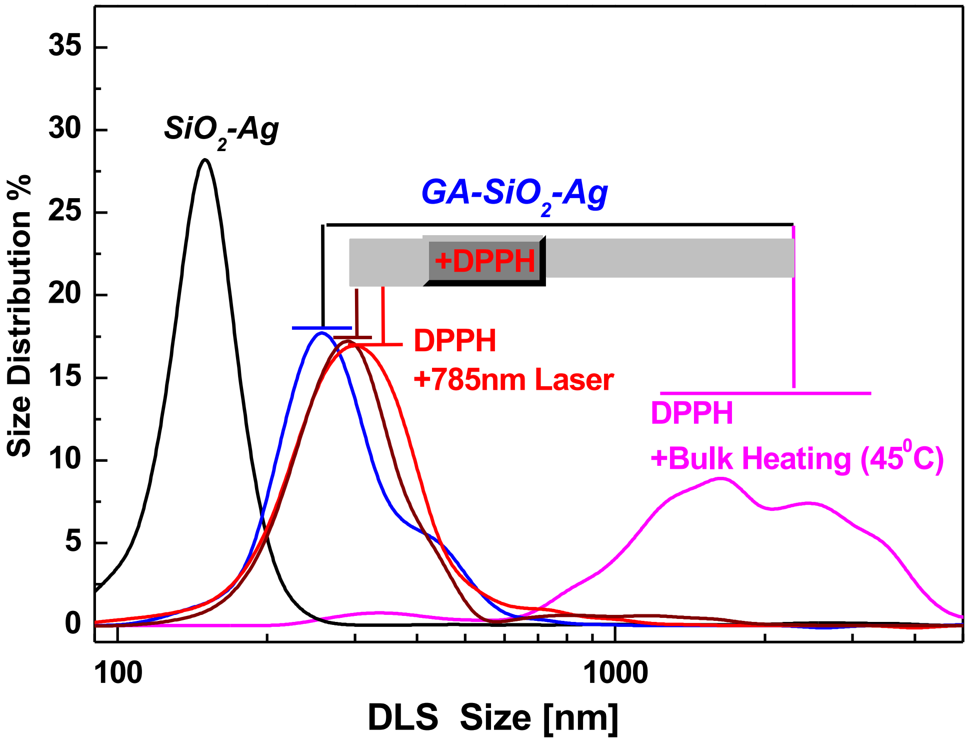

Figure S3. Dynamic light scattering (DLS) number distributions of as-prepared SiO_2-coated Ag NPs (black line) and GA functionalized SiO_2-coated Ag NPs (blue line) in the presence of DPPH (crimson line), in the presence of DPPH and under 785 nm irradiation for 30 minutes (red line) or bulk-heating at 45 ˚C for 30 minutes (magenta line).

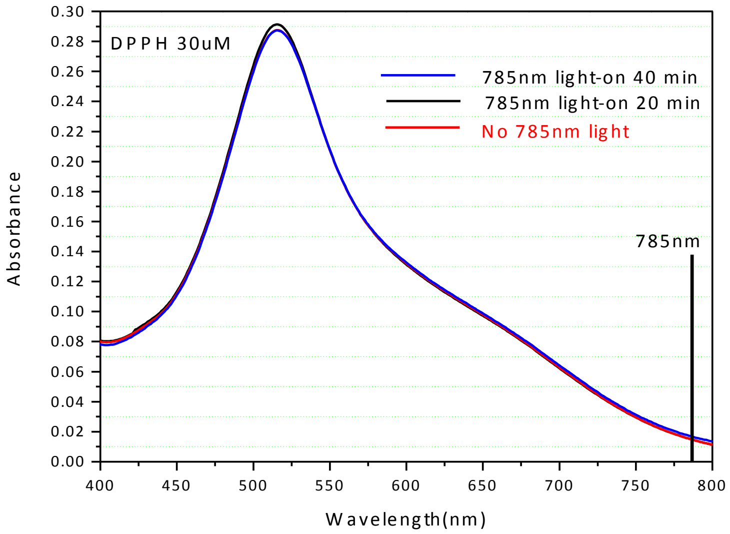

Figure S4. UV-Vis absorbance spectrum for 30 µM DPPH radicals in methanol. The spectra have been recorded under no-light irradiation (red line), or after 20 minutes (black line) or 40 minutes (blue line) under 785 nm laser irradiation. The data show that under these conditions 785 nm laser irradiation had no effect on the DPPH radicals.

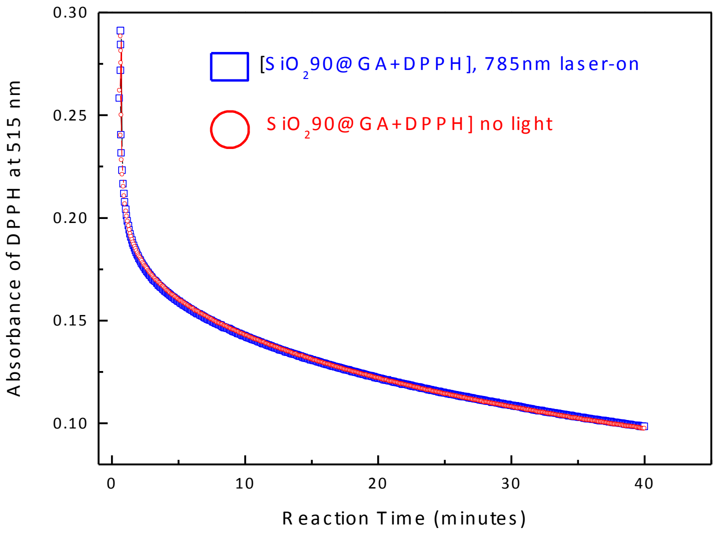

Figure S5. Kinetics of the absorbance of 30µM DPPH radicals at 515 nm in the presence of $SiO_2$90@GA particles (corresponding to a concentration of 4µM of GA). The spectra have been recorded under no-light irradiation (red symbols), or under 785 nm laser irradiation (blue symbols). The data show that under these conditions 785 nm laser irradiation had no effect on the kinetics of the DPPH radical decay via the HAT mechanism.

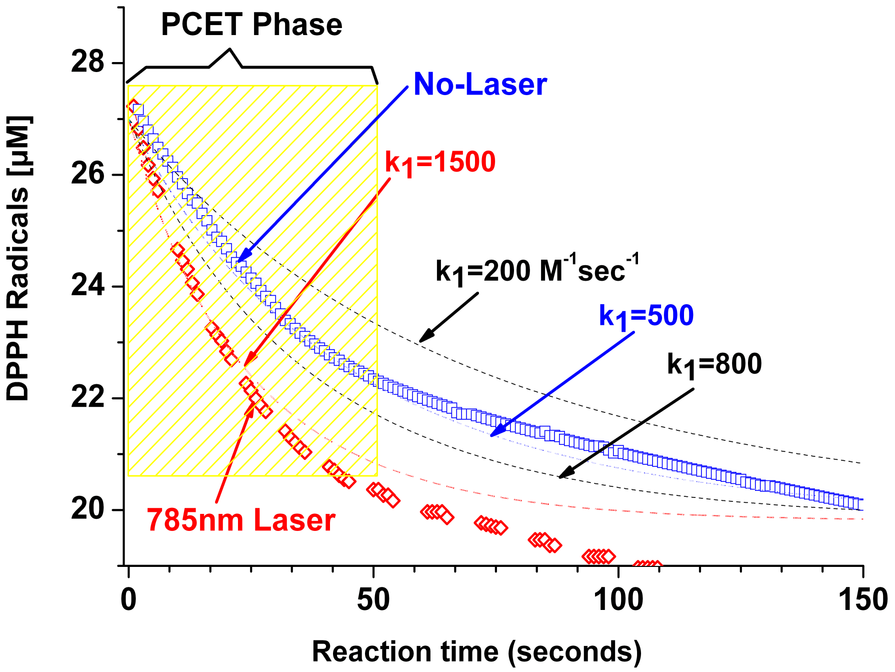

Figure S6. Kinetic traces of DPPH radical quenching by GA functionalized SiO_2-coated Ag NPs with (red symbols) and without (blue symbols) 785 nm laser irradiation. The dashed lines are theoretical simulations using equation (1) for various kinetic rates k_1 as indicated. The yellow frame marks the initial fast phase of the DPPH radical quenching that corresponds to the HAT from the OH groups of GA to DPPH radicals.

We have carefully examined the possible effect of excessive 785 nm laser power during Raman spectroscopy on the integrity of the GA molecules since strong laser power might easily cause severe damage to the organics.[2] At laser power >0.5 mW, the gallic bands (~1200-1600 cm^{-1}) start to deteriorate (Figure S5, blue line), indicating thermal decomposition of GA. This has also been observed for SERS of GA[3] and numerous other organics[2] on metallic silver.

At higher laser power (>5 mW), the characteristic "carbon cathedral"[2] at ~1580 cm^{-1} appears (Figure S5) that is a well known manifestation of strong thermal carbonisation of GA on the SiO_2-coated Ag nanoparticles. The lowest laser power used in the Raman experiments (0.05 mW, 5x objective, NA = 0.12) (Figure 4) corresponds to radiative flux of 100 W/cm^2, much higher than those used for the plasmon enhanced HAT reaction (Figure 3a). Thus the 785 nm laser irradiation power used during the HAT reaction (11.7 W/cm^2, Figure 3) should not destroy any GA molecule. This is supported here also by the good antioxidant activity of the GA functionalized SiO_2-coated Ag nanoparticles (Figure 3).

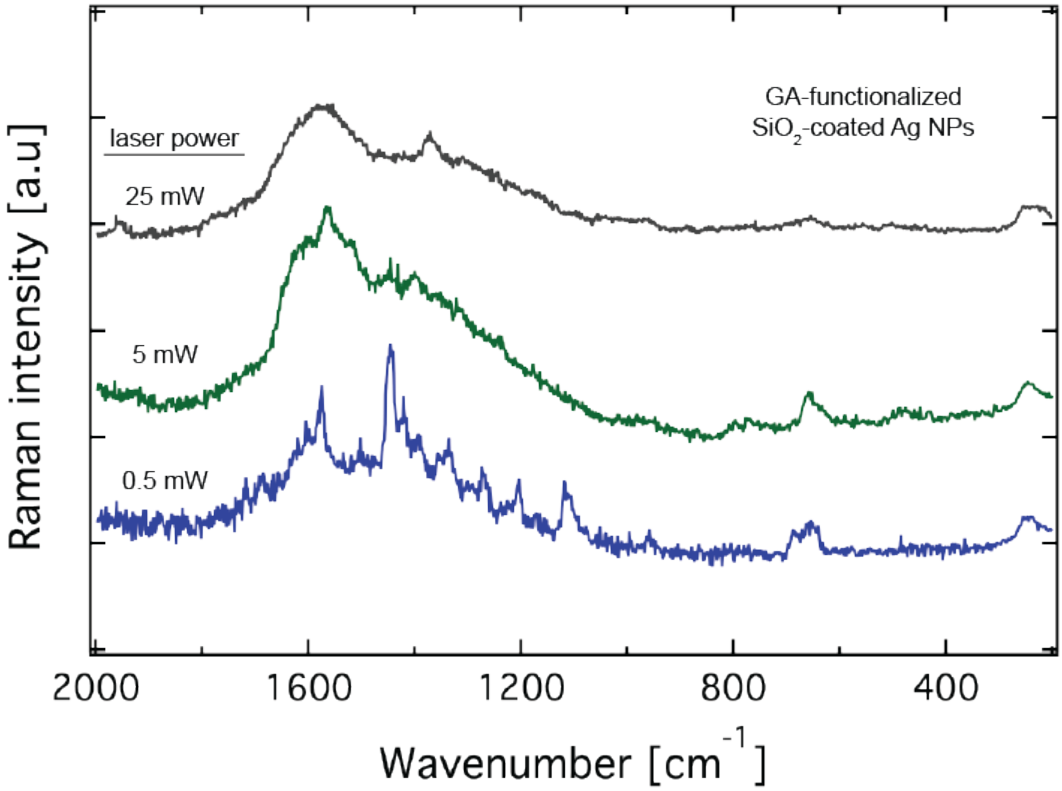

Figure S7. Raman spectra for GA functionalized SiO_2-coated Ag NPs recorded using a 785 nm laser excitation at various powers.

Energetic considerations

Bond dissociation enthalpies (BDE) have been shown to determine the HAT antiradical activity of phenolic antioxidants. BDE correspond to the enthalpy change for the reaction (equation 1):[4]

$$\mathrm{ArO\text{-}H} \rightarrow \mathrm{ArO}^{\bullet} + \mathrm{H}^{\bullet} \qquad (1)$$

In order to provide an exoergic, and therefore rapid reaction, an antioxidant (ArO-H) interacting with a radical (X), should have a BDE below that the BDE of X-H. The lower the BDE of ArO-H, the faster the HAT reaction is, resulting in better antioxidant performance.

Detailed experimental and theoretical data kinetic are available for $DPPH^{\bullet}$ scavenging by phenolics in homogeneous phase[5-7] as well as for phenolics attached on polymers[8,9] or SiO_2 nanoparticles.[1] These data, which cover nearly four orders of magnitude in kinetic rates of $DPPH^{\bullet}$ scavenging, provide convincing evidence for a linear correlation between BDEs (kcal mol^{-1}) *vs.* the log of the kinetic constant k_1 (in $M^{-1}s^{-1}$) (equation 2):

$$\mathrm{BDE\ (kcal/mol)} \sim C_1 - C_2 \times \log(k_1) \qquad (2)$$

with C_1~90-100 and C_2~3. This includes data of Wright et al. in ethyl acetate,[7] by Foti et al. in heptanes[10] and Kawashima et al. in acetonitrile and methanol.[11,12] Equation (2) shows that BDE is very sensitive to k_1 values: for example, lowering of BDE by 1 kcal/mole will be easily detected as a faster HAT kinetic constant by a factor of 2.[7,13,14] In this context, the kinetic rates *vs.* the 785 nm laser radiative flux in Figure 3d, confirm that for higher laser radiative flux, faster k_1 are obtained that correspond to lower BDE for the OH groups of GA towards DPPH.

From the data in Figure 3d, the k_1 rates in equation (2) can be attributed to a decrease of BDE by at least 2 kcal/mol. Using the linear relationship between E_a(= activation energy of HAT) and BDE, as shown by Foti et al[4], we conclude that a change of BDE (GA-OH) by 2 kcal/mole gives a decrease of the activation energy ΔE_a ~1.8 kcal/mole. A simple calculation shows that this amount of energy cannot be attributed to bulk heating effect (at T=298 K, RT=0.58 kcal/mole, thus RT = 1.8 kcal/mole corresponds to T = 924 K). Such a high local temperature would result in degradation of the grafted GA e.g. since thermogravimetric data show that grafted GA moieties are thermally decomposed a T=400 °C.[14]

In conclusion, the present data and their analysis cannot be accounted by a bulk heating effect. This is also supported by our Raman data (Figure 4 and Figure S5) which show that low-power near-IR 785 nm laser irradiation on GA-functionalized SiO_2-coated Ag nanoparticles induces Raman enhancement of GA, with *no thermal decomposition* events. The locally generated heat is probably dissipated by the methanol solvent molecules as evidenced by the thermal camera temperature data.

Overall, this analysis provides a straightforward explanation of the observed enhancement of the HAT caused by the near-IR 785nm laser:

[i] GA-functionalized SiO_2-coated Ag nanoparticles show enhanced plasmonic response at near-IR wavelengths due to particle agglomeration caused by the GA molecules.

[ii] 785 nm laser irradiation induces strong hot-spots by exciting surface plasmonic resonances of the coupled nanoparticles as directly detected by SERS of the GA molecules.[15,16]

[iii] The surface enhanced plasmon resonances lower the GA-OH bond dissociation enthalpies by at least 2 kcal/mole.

[iv] Ultimately, it is this lower $BDE_{(GA\text{-}OH)}$ that enhances dramatically the HAT rates to $DPPH^{\bullet}$ and therefore improves the antioxidant activity.

This is the first experimental example of bridging two fundamental - so far unrelated - phenomena: *hot-spots created by surface plasmon resonance* can enhance *Hydrogen Atom Tranfer* from a phenolic OH to DPPH$^\bullet$.

Mechanism of Plasmon-Enhanced PCET

The interaction of an excited plasmonic metallic particle with an organic molecule can occur *via* two main mechanisms: (a) chemical, and (b) electromagnetic.[17,18] The chemical mechanism requires a direct contact of the molecule with the metallic nanoparticle surface.[19,20] Here, for the core-shell SiO_2 coated Ag nanoparticles, this chemical mechanism is not very likely because the nanolayer of SiO_2 prevents direct contact of GA or DPPH with the Ag nanoparticle. On the other hand, the electromagnetic mechanism is more likely the reason we observe the enhanced antioxidant activity here i.e. because the local electric field at the nanoparticle surface vicinity and at GA molecule position, is greatly amplified during the plasmon excitation. In fact, plasmonic enhancements up to 10^4-10^8 fold are commonly reported.[17,18] In aggregates of plasmonic nanoparticles, these local electric fields are evanescent *i.e.* non propagating, and are localized within few nanometers from the nanoparticle surface.[21] In this context, Shanthil et al.[15] provided experimental evidence that strong local electric field gradients -or hot spots- are efficiently generated in aggregated SiO_2-coated Ag nanoparticles.

To connect the plasmonic local field with the PCET we consider two main factors. First, the formation of an activated transient state where the phenolic molecule and DPPH$^\bullet$ come to close proximity. This has been established by numerous previous studies.[4,22,23] Second, involvement of solvent molecules in PCET from the OH group of GA to DPPH$^\bullet$.[4,7,14,23] Both experimental and quantum chemical calculations show that HAT from gallate derivatives to DPPH$^\bullet$ is strongly favoured in methanol *vs.* other solvents such as acetone or THF.[22] Energetically, methanol has been shown to lower the activation energy E_a of HAT reaction, see Scheme 1a in main manuscript.[22]

In this context, we consider that the observed plasmon-enhancement PCET from GA to DPPH is due to local, evanescent, electric fields localized in the vicinity of the grafted GA molecules (Scheme 1b in main manuscript). Since the Ag nanoparticles that serve as the source of evanescent light are smaller than the 785 nm wavelengh, then the GA molecules - as well as nearby solvent MetOH molecules - sense the local electric field vibrations. This causes distortion within the molecules that generates lattice vibrations (phonons) that may have two effects. First, generate oscillating electric dipoles[21] on GA and/or nearby MetOH molecules. The strong SERS effect detected by Raman on GA (Figure 4) is a direct manifestation of these local electric field oscillations on the vibrational properties of GA. We consider that the oscillating local electric field can have a strong interaction with methanol molecules, since methanol is a polar organic $\varepsilon = 32.7$, and activate them.[24,25] Second effect of the local electric fields is the energy dissipation as heat *via* non-radiative processes.[26,27] Figure 2 shows that 785 nm laser irradiation is indeed capable to generate heat raising the bulk temperature of the reaction mixture by more than 30 ˚C. On the other hand, the DPPH quenching data show that this bulk heating is *not* the dominant mechanism that determines the observed acceleration of PCET under 785 nm irradiation. Although bulk heating may have a beneficial effect on PCET from GA to DPPH at short reaction times, it eventually has strong adverse effects due to radical-induced particle agglomeration (Supplementary Information, Figure S3) that ultimately would deactivate HAT.

On the other hand, in contrast to the bulk heating mechanism, the electric oscillation enhancement is a *local* phenomenon that operates within few nanometers from the particle surface.[15,21] Taking into account the Raman enhancement on GA, we consider that the local electrical oscillations are the main reason for the decrease of BDE by 2 kcal/mole and the activation barrier by $\Delta E_a = -1.8$ kcal/mole. This is visualized in Scheme 1b in main manuscript where we assume that local oscillations affect both GA as well as the vicinal MetOH solvent molecules, decreasing the activation energy barrier for the PCET.

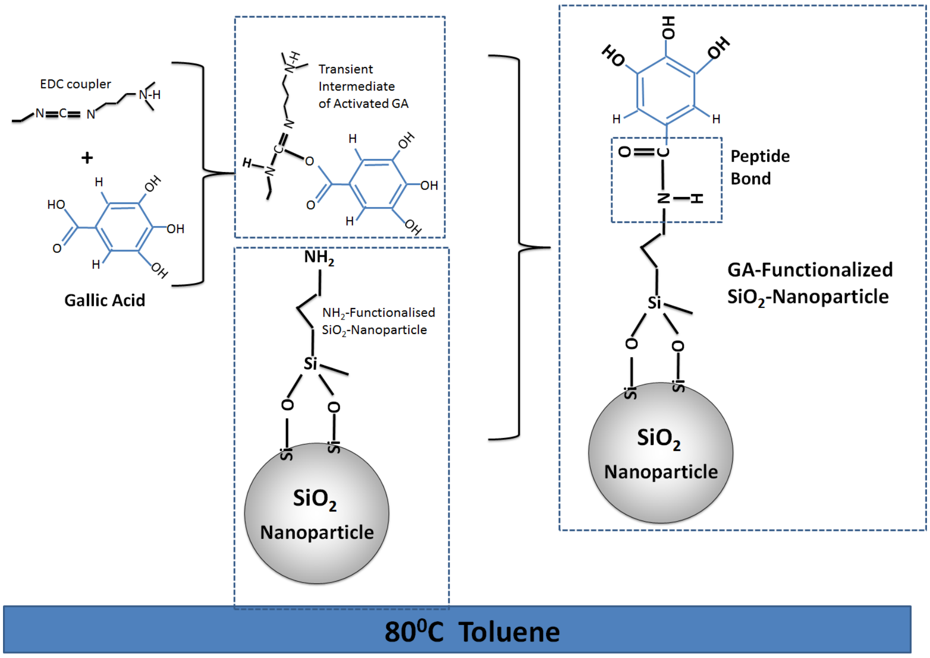

Scheme S1. The functionalization steps used in this study.

References

1. Y. Deligiannakis, G. A. Sotiriou & S. E. Pratsinis. Antioxidant and Antiradical SiO$_2$ Nanoparticles Covalently Functionalized with Gallic Acid. *ACS Appl. Mater. Interfaces* **4**, 6609-6617 (2012).
2. R. A. Alvarez-Puebla. Effects of the Excitation Wavelength on the SERS Spectrum. *J. Phys. Chem. Lett.* **3**, 857-866 (2012).
3. S. Sanchez-Cortes & J. V. Garcia-Ramos. Adsorption and chemical modification of phenols on a silver surface. *J. Colloid Interface Sci.* **231**, 98-106 (2000).
4. M. C. Foti, C. Daquino, I. D. Mackie, G. A. DiLabio & K. U. Ingold. Reaction of Phenols with the 2,2-Diphenyl-1-picrylhydrazyl Radical. Kinetics and DFT Calculations Applied To Determine ArO-H Bond Dissociation Enthalpies and Reaction Mechanism. *J. Org. Chem.* **73**, 9270-9282 (2008).
5. M. C. Foti, C. Daquino, G. A. DiLabio & K. U. Ingold. Kinetics of the Oxidation of Quercetin by 2,2-Diphenyl-1-picrylhydrazyl (DPPH●). *Org. Lett.* **13**, 4826-4829 (2011).
6. G. Litwinienko & K. U. Ingold. Abnormal solvent effects on hydrogen atom abstraction. 3. Novel kinetics in sequential proton loss electron transfer chemistry. *J. Org. Chem.* **70**, 8982-8990 (2005).
7. J. S. Wright, E. R. Johnson & G. A. DiLabio. Predicting the activity of phenolic antioxidants: Theoretical method, analysis of substituent effects, and application to major families of antioxidants. *J. Am. Chem. Soc.* **123**, 1173-1183 (2001).
8. Y.-S. Cho, S.-K. Kim, C.-B. Ahn & J.-Y. Je. Preparation, characterization, and antioxidant properties of gallic acid-grafted-chitosans. *Carbohydr. Polym.* **83**, 1617-1622 (2011).
9. W. Pasanphan, G. R. Buettner & S. Chirachanchai. Chitosan conjugated with deoxycholic acid and gallic acid: A novel biopolymer-based additive antioxidant for polyethylene. *J. Appl. Polym. Sci.* **109**, 38-46 (2008).
10. M. C. Foti, E. R. Johnson, M. R. Vinqvist, J. S. Wright, L. R. C. Barclay & K. U. Ingold. Naphthalene diols: A new class of antioxidants intramolecular hydrogen bonding in catechols, naphthalene diols, and their aryloxyl radicals. *J. Org. Chem.* **67**, 5190-5196 (2002).
11. T. Kawashima *et al.* Kinetics and Mechanism for the Scavenging Reaction of the 2,2-Diphenyl-1-picrylhydrazyl Radical by Synthetic Artepillin C Analogues. *Bull. Chem. Soc. Jpn.* **85**, 877-883 (2012).
12. T. Kawashima, K. Ohkubo & S. Fukuzumi. Radical Scavenging Reactivity of Catecholamine Neurotransmitters and the Inhibition Effect for DNA Cleavage. *J. Phys. Chem. B* **114**, 675-680 (2010).

13. M. Lucarini, G. F. Pedulli & M. Cipollone. Bond-dissociation enthalpy of alpha-tocopherol and other phenolic antioxidants. *J. Org. Chem.* **59**, 5063-5070 (1994).
14. D. D. M. Wayner, E. Lusztyk, D. Page, K. U. Ingold, P. Mulder & L. J. J. Laarhoven. Effects of solvation on the enthaplies of reaction of tert-butoxyl radicals with phenol and on the calculated O-H bond strength in phenol. *J. Am. Chem. Soc.* **117**, 8737-8744 (1995).
15. M. Shanthil, R. Thomas, R. S. Swathi & K. George Thomas. Ag@SiO_2 Core-Shell Nanostructures: Distance-Dependent Plasmon Coupling and SERS Investigation. *J. Phys. Chem. Lett.* **3**, 1459-1464 (2012).
16. C.-W. Yen & M. A. El-Sayed. Plasmonic Field Effect on the Hexacyanoferrate (III)-Thiosulfate Electron Transfer Catalytic Reaction on Gold Nanoparticles: Electromagnetic or Thermal? *J. Phys. Chem. C* **113**, 19585-19590 (2009).
17. J. Gersten & A. Nitzan. Electromagnetic theory of enhanced Raman-scattering by molecules adsorbed on rough surfaces. *J. Chem. Phys.* **73**, 3023-3037 (1980).
18. G. Schatz, M. Young & R. Duyne. in *Surface-Enhanced Raman Scattering* Vol. 103 *Topics in Applied Physics* (eds Katrin Kneipp, Martin Moskovits, & Harald Kneipp) Ch. 2, 19-45 (Springer Berlin Heidelberg, 2006).
19. S. M. Morton & L. Jensen. Understanding the Molecule-Surface Chemical Coupling in SERS. *J. Am. Chem. Soc.* **131**, 4090-4098 (2009).
20. P. Christopher, H. Xin & S. Linic. Visible-light-enhanced catalytic oxidation reactions on plasmonic silver nanostructures. *Nat. Chem.* **3**, 467-472 (2011).
21. K. A. Willets & R. P. Van Duyne. Localized surface plasmon resonance spectroscopy and sensing. *Annu. Rev. Phys. Chem.* **58**, 267-297 (2007).
22. V. Thavasi, R. P. A. Bettens & L. P. Leong. Temperature and Solvent Effects on Radical Scavenging Ability of Phenols. *J. Phys. Chem. B* **113**, 3068-3077 (2009).
23. D. R. Weinberg *et al.* Proton-Coupled Electron Transfer. *Chem. Rev.* **112**, 4016-4093 (2012).
24. X. Chen, H.-Y. Zhu, J.-C. Zhao, Z.-T. Zheng & X.-P. Gao. Visible-light-driven oxidation of organic contaminants in air with gold nanoparticle catalysts on oxide supports. *Angew. Chem.-Int. Edit.* **47**, 5353-5356 (2008).
25. X. Zhang, Y. L. Chen, R.-S. Liu & D. P. Tsai. Plasmonic photocatalysis. *Rep. Prog. Phys.* **76**, (2013).
26. D. D. Evanoff & G. Chumanov. Synthesis and optical properties of silver nanoparticles and arrays. *ChemPhysChem* **6**, 1221-1231 (2005).
27. K. L. Kelly, E. Coronado, L. L. Zhao & G. C. Schatz. The optical properties of metal nanoparticles: The influence of size, shape, and dielectric environment. *J. Phys. Chem. B* **107**, 668-677 (2003).